



PUBLISHED FOR SISSA BY SPRINGER

RECEIVED: January 28, 2015

ACCEPTED: March 17, 2015

PUBLISHED: April 9, 2015

Measurement of indirect CP asymmetries in $D^0 \rightarrow K^- K^+$ and $D^0 \rightarrow \pi^- \pi^+$ decays using semileptonic B decays



The LHCb collaboration

E-mail: Jeroen.van.Tilburg@cern.ch

ABSTRACT: Time-dependent CP asymmetries in the decay rates of the singly Cabibbo-suppressed decays $D^0 \rightarrow K^- K^+$ and $D^0 \rightarrow \pi^- \pi^+$ are measured in pp collision data corresponding to an integrated luminosity of 3.0 fb^{-1} collected by the LHCb experiment. The D^0 mesons are produced in semileptonic b -hadron decays, where the charge of the accompanying muon is used to determine the initial state as D^0 or \bar{D}^0 . The asymmetries in effective lifetimes between D^0 and \bar{D}^0 decays, which are sensitive to indirect CP violation, are determined to be

$$A_{\Gamma}(K^- K^+) = (-0.134 \pm 0.077^{+0.026}_{-0.034}) \%,$$
$$A_{\Gamma}(\pi^- \pi^+) = (-0.092 \pm 0.145^{+0.025}_{-0.033}) \%,$$

where the first uncertainties are statistical and the second systematic. This result is in agreement with previous measurements and with the hypothesis of no indirect CP violation in D^0 decays.

KEYWORDS: CP violation, Charm physics, Lifetime, Hadron-Hadron Scattering

ARXIV EPRINT: [1501.06777](https://arxiv.org/abs/1501.06777)

Contents

1	Introduction	1
2	Formalism and method	2
3	Detector and simulation	3
4	Data set and selection	3
5	Determination of A_Γ	4
6	Systematic uncertainties and consistency checks	7
7	Conclusions	9
	The LHCb collaboration	14

1 Introduction

In neutral meson systems, mixing may occur between the particle and anti-particle states. This mixing is very small in the charm-meson (D^0) system. Experimentally, a small, non-zero D^0 – \bar{D}^0 mixing is now firmly established by several experiments [1–6], where the average of these measurements excludes zero mixing at more than 11 standard deviations [7]. This opens up the possibility to search for a breaking of the charge-parity (CP) symmetry occurring in the D^0 – \bar{D}^0 mixing alone or in the interference between the mixing and decay amplitudes. This is called indirect CP violation and the corresponding asymmetry is predicted to be $\mathcal{O}(10^{-4})$ [8, 9], but can be enhanced in theories beyond the Standard Model [10]. Indirect CP violation can be measured in decays to CP eigenstates such as the singly Cabibbo-suppressed decays $D^0 \rightarrow K^- K^+$ and $D^0 \rightarrow \pi^- \pi^+$ (the inclusion of charge-conjugate processes is implied hereafter) from the asymmetry between the effective D^0 and \bar{D}^0 lifetimes, A_Γ . The effective lifetime is the lifetime obtained from a single exponential fit to the decay-time distribution. Several measurements of A_Γ exist [1, 11, 12]. The most precise determination was made by LHCb with data corresponding to 1.0 fb^{-1} of integrated luminosity, resulting in $A_\Gamma(K^- K^+) = (-0.035 \pm 0.062 \pm 0.012)\%$, and $A_\Gamma(\pi^- \pi^+) = (0.033 \pm 0.106 \pm 0.014)\%$ [11]. When indirect CP violation is assumed to be the same in the two modes, the world average becomes $A_\Gamma = (-0.014 \pm 0.052)\%$ [7]. In all previous measurements of A_Γ , the initial flavour of the neutral charm meson (i.e., whether it was a D^0 or \bar{D}^0 state) was determined (tagged) by the charge of the pion in a $D^{*+} \rightarrow D^0 \pi^+$ decay. In this paper, the time-dependent CP asymmetry is measured in D^0

decays originating from semileptonic b -hadron decays, where the charge of the accompanying muon is used to tag the flavour of the D^0 meson. These samples are dominated by $B^- \rightarrow D^0 \mu^- \bar{\nu}_\mu X$ and $\bar{B}^0 \rightarrow D^0 \mu^- \bar{\nu}_\mu X$ decays, where X denotes other particle(s) possibly produced in the decay. The same data samples as for the measurement of time-integrated CP asymmetries [13] are used.

2 Formalism and method

The time-dependent CP asymmetry for a neutral D meson decaying to a CP eigenstate, f , is defined as

$$A_{CP}(t) \equiv \frac{\Gamma(D^0 \rightarrow f; t) - \Gamma(\bar{D}^0 \rightarrow f; t)}{\Gamma(D^0 \rightarrow f; t) + \Gamma(\bar{D}^0 \rightarrow f; t)}, \quad (2.1)$$

where $\Gamma(D^0 \rightarrow f; t)$ and $\Gamma(\bar{D}^0 \rightarrow f; t)$ are the time-dependent partial widths of initial D^0 and \bar{D}^0 mesons to final state f . The CP asymmetry can be approximated as [14]

$$A_{CP}(t) \approx A_{CP}^{\text{dir}} - A_\Gamma \frac{t}{\tau}, \quad (2.2)$$

where A_{CP}^{dir} is the direct CP asymmetry and τ is the D^0 lifetime. The linear decay-time dependence is determined by A_Γ , which is formally defined as

$$A_\Gamma \equiv \frac{\hat{\Gamma}_{D^0} - \hat{\Gamma}_{\bar{D}^0}}{\hat{\Gamma}_{D^0} + \hat{\Gamma}_{\bar{D}^0}}, \quad (2.3)$$

where $\hat{\Gamma}$ is the effective partial decay rate of an initial D^0 or \bar{D}^0 state to the CP eigenstate. Furthermore, A_Γ can be approximated in terms of the D^0 – \bar{D}^0 mixing parameters, x and y , as [15]

$$A_\Gamma \approx \left(A_{CP}^{\text{mix}}/2 - A_{CP}^{\text{dir}} \right) y \cos \phi - x \sin \phi, \quad (2.4)$$

where $A_{CP}^{\text{mix}} = |q/p|^2 - 1$ describes CP violation in D^0 – \bar{D}^0 mixing, with q and p the coefficients of the transformation from the flavour basis to the mass basis, $|D_{1,2}\rangle = p|D^0\rangle \pm q|\bar{D}^0\rangle$. The weak phase ϕ describes CP violation in the interference between mixing and decay, and is specific to the decay mode. Finally, A_Γ receives a contribution from direct CP violation as well [16].

The raw asymmetry is affected by the different detection efficiencies for positive and negative muons, and the different production rates of D^0 and \bar{D}^0 mesons. These effects introduce a shift to the constant term in eq. (2.2), but have a negligible effect on the measurement of A_Γ (see section 6). The decay $D^0 \rightarrow K^- \pi^+$, also flavour-tagged by the muon from a semileptonic b -hadron decay, is used as a control channel. Since this is a Cabibbo-favoured decay mode, direct CP violation is expected to be negligible. More importantly, any indirect CP violation is heavily suppressed as the contribution from doubly Cabibbo-suppressed $D^0 \rightarrow K^+ \pi^-$ decays is small.

3 Detector and simulation

The LHCb detector [17, 18] is a single-arm forward spectrometer covering the pseudo-rapidity range $2 < \eta < 5$, designed for the study of particles containing b or c quarks. The detector includes a high-precision tracking system consisting of a silicon-strip vertex detector surrounding the pp interaction region, a large-area silicon-strip detector located upstream of a dipole magnet with a bending power of about 4 Tm, and three stations of silicon-strip detectors and straw drift tubes placed downstream of the magnet. The polarity of the magnetic field is regularly reversed during data taking. The tracking system provides a measurement of momentum, p , with a relative uncertainty that varies from 0.5% at low momentum to 1.0% at 200 GeV/ c . The minimum distance of a track to a primary vertex, the impact parameter, is measured with a resolution of $(15 + 29/p_T) \mu\text{m}$, where p_T is the component of the momentum transverse to the beam, in GeV/ c . Different types of charged hadrons are distinguished using information from two ring-imaging Cherenkov detectors. Photon, electron and hadron candidates are identified by a calorimeter system consisting of scintillating-pad and preshower detectors, an electromagnetic calorimeter and a hadronic calorimeter. Muons are identified by a system composed of alternating layers of iron and multiwire proportional chambers, situated behind the hadronic calorimeter. The trigger [19] consists of a hardware stage, based on information from the calorimeter and muon systems, followed by a software stage, which applies a full event reconstruction.

In the simulation, pp collisions are generated using PYTHIA [20, 21] with a specific LHCb configuration [22]. Decays of hadronic particles are described by EVTGEN [23], in which final-state radiation is generated using PHOTOS [24]. The interaction of the generated particles with the detector, and its response, are implemented using the GEANT4 toolkit [25, 26] as described in ref. [27].

4 Data set and selection

This analysis uses a data set corresponding to an integrated luminosity of 3.0 fb^{-1} . The data were taken at two different pp centre-of-mass energies: 7 TeV in 2011 (1.0 fb^{-1}) and 8 TeV in 2012 (2.0 fb^{-1}). The data sets recorded with each dipole magnet polarity are roughly equal in size.

At the hardware trigger stage, the events are triggered by the presence of the muon candidate in the muon system. This requires the muon p_T to be greater than 1.64 GeV/ c (1.76 GeV/ c) for the 2011 (2012) data. At the software trigger stage, one of the final-state particles is required to have enough momentum and be significantly displaced from any primary pp vertex. In addition, the candidates must be selected by a single-muon trigger or by a topological trigger that requires the muon and one or two of the D^0 daughters to be consistent with the topology of b -hadron decays [19].

To further suppress background, the D^0 daughters are required to have $p_T > 300 \text{ MeV}/c$. All final-state particles are required to have a large impact parameter and be well identified by the particle identification systems. The impact parameter requirement on the muon reduces the contribution from D^0 mesons produced directly in the pp interaction to below 2%. The scalar p_T sum of the D^0 daughters should be larger than 1.4 GeV/ c , and the p_T of

the D^0 candidate should be larger than $0.5 \text{ GeV}/c$. The two tracks from the D^0 candidate and the $D^0\mu$ combination are required to form good vertices and the latter vertex should be closer to the primary vertex than the D^0 vertex. The D^0 decay time is determined from the distance between these two vertices, and the reconstructed D^0 momentum. The invariant mass of the $D^0\mu$ combination is required to be between 2.5 and $5.0 \text{ GeV}/c^2$, where the upper bound suppresses hadronic b -hadron decays into three-body final states. Backgrounds from inclusive b -hadron decays into charmonium are suppressed by vetoing candidates where the invariant mass of the muon and the oppositely charged D^0 daughter, misidentified as a muon, is consistent with the J/ψ or $\psi(2S)$ mass. Additionally, the invariant mass of the muon and same-charge D^0 daughter, under the muon mass hypothesis, is required to be larger than $240 \text{ MeV}/c^2$ to remove events where a single charged particle is reconstructed as two separate tracks. For most selection requirements, the efficiency is roughly independent of the D^0 decay time, giving efficiency variations of $\mathcal{O}(1\%)$. The largest dependence on the decay time comes from the topological trigger, which introduces an efficiency profile that decreases with D^0 decay time, resulting in about 20% relative efficiency loss at large decay times.

5 Determination of A_{Γ}

The mass distributions for the selected $D^0 \rightarrow K^-K^+$, $D^0 \rightarrow \pi^-\pi^+$ and $D^0 \rightarrow K^-\pi^+$ candidates are shown in figure 1. The numbers of signal candidates are determined from unbinned extended maximum-likelihood fits in the range 1810 to $1920 \text{ MeV}/c^2$. The signal for all three decay modes is modelled by a sum of three Gaussian functions. The first two have the same mean, but independent widths; the third is used to describe a small radiative tail, and has a lower mean and larger width. The effective width of the signal ranges from $7.1 \text{ MeV}/c^2$ for $D^0 \rightarrow K^-K^+$ candidates to $9.3 \text{ MeV}/c^2$ for $D^0 \rightarrow \pi^-\pi^+$ candidates. As the final states K^-K^+ and $\pi^-\pi^+$ are charge symmetric, the shape parameters for the signal are the same for both D^0 and \bar{D}^0 candidates. The combinatorial background is modelled by an exponential function. In the $\pi^-\pi^+$ invariant mass distribution, a reflection from $D^0 \rightarrow K^-\pi^+$ decays is visible in the region below $1820 \text{ MeV}/c^2$. This background component is modelled by a single Gaussian function and the fit range is extended from 1795 to $1930 \text{ MeV}/c^2$. The shape parameters and overall normalisation of the background components are allowed to differ between D^0 and \bar{D}^0 candidates. The numbers of signal candidates obtained from these global fits are 2.34×10^6 for $D^0 \rightarrow K^-K^+$, 0.79×10^6 for $D^0 \rightarrow \pi^-\pi^+$ and 11.31×10^6 for $D^0 \rightarrow K^-\pi^+$ decays. The latter number corresponds to only half of the available $D^0 \rightarrow K^-\pi^+$ candidates, randomly selected, to reduce the sample size.

The raw CP asymmetry is determined from fits to the mass distributions in 50 bins of the D^0 decay time. The fits are performed simultaneously for D^0 and \bar{D}^0 candidates and the asymmetry is determined for each decay-time bin. The shape parameters and relative normalisation for the third Gaussian function and for the $D^0 \rightarrow K^-\pi^+$ reflection background are fixed from the global fit. All other parameters are allowed to vary in these fits. In particular, since both the amount and the composition of background depend on the decay time, the background parameters are free to vary in each decay-time bin. For decay times larger than 1 ps the relative contribution from combinatorial background increases.

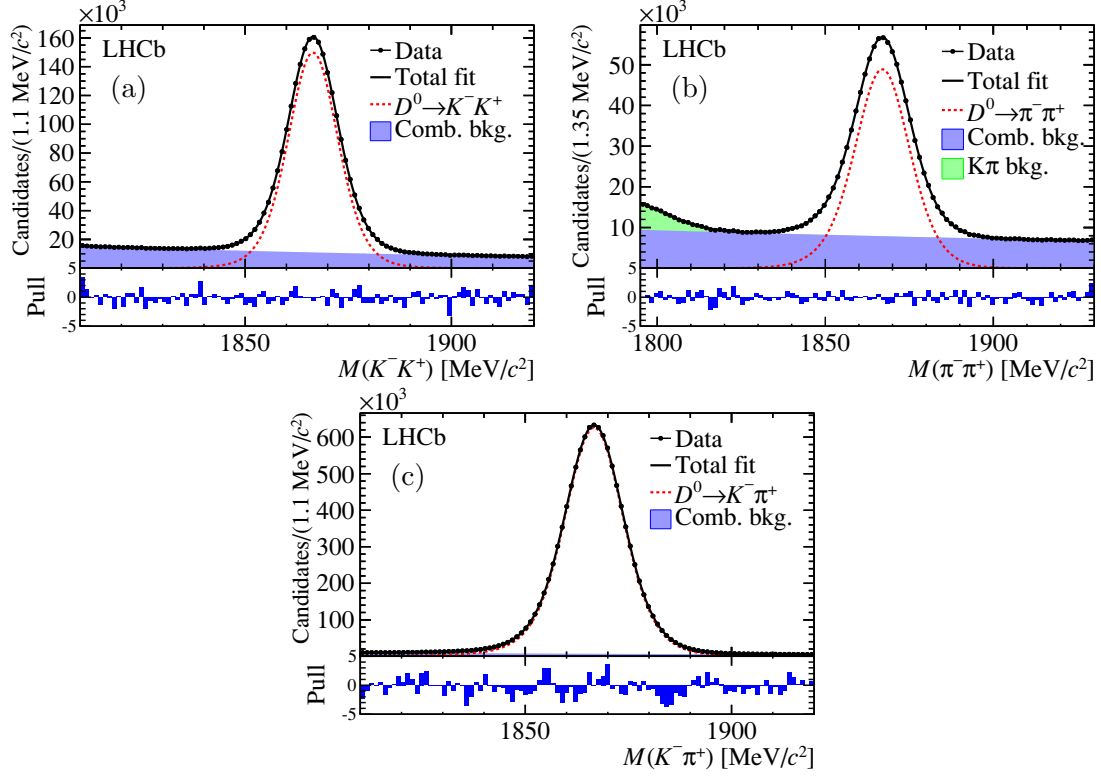


Figure 1. Invariant mass distributions for (a) $D^0 \rightarrow K^- K^+$, (b) $D^0 \rightarrow \pi^- \pi^+$ and (c) $D^0 \rightarrow K^- \pi^+$ candidates. The results of the fits are overlaid. Underneath each plot the pull in each mass bin is shown, where the pull is defined as the difference between the data point and total fit, divided by the corresponding uncertainty.

This is due to the exponential decrease of the signal and a less steep dependence of the combinatorial background on the decay time. The mass distribution in each decay-time bin is well described by the model.

Events at large D^0 decay times have a larger sensitivity to A_Γ compared to events at small decay times, which is balanced by the fewer signal candidates at large decay times. The binning in D^0 decay time is chosen such that every bin gives roughly the same statistical contribution to A_Γ . The value of A_Γ is determined from a χ^2 fit to the time-dependent asymmetry of eq. (2.2). The value of A_Γ and the offset in the asymmetry are allowed to vary in the fit, while the D^0 lifetime is fixed to $\tau = 410.1$ fs [28]. Due to the exponential decay-time distribution, the average time in each bin is not in the centre of the bin. Therefore, the background-subtracted [29] average decay time is determined in each bin and used in the fit. This fit procedure gives unbiased results and correct uncertainties, as is verified by simulating many experiments with large samples.

The measured asymmetries in bins of decay time are shown in figure 2, including the result of the time-dependent fit. The results in the three decay channels are

$$\begin{aligned} A_\Gamma(K^- K^+) &= (-0.134 \pm 0.077)\%, \\ A_\Gamma(\pi^- \pi^+) &= (-0.092 \pm 0.145)\%, \\ A_\Gamma(K^- \pi^+) &= (0.009 \pm 0.032)\%, \end{aligned}$$

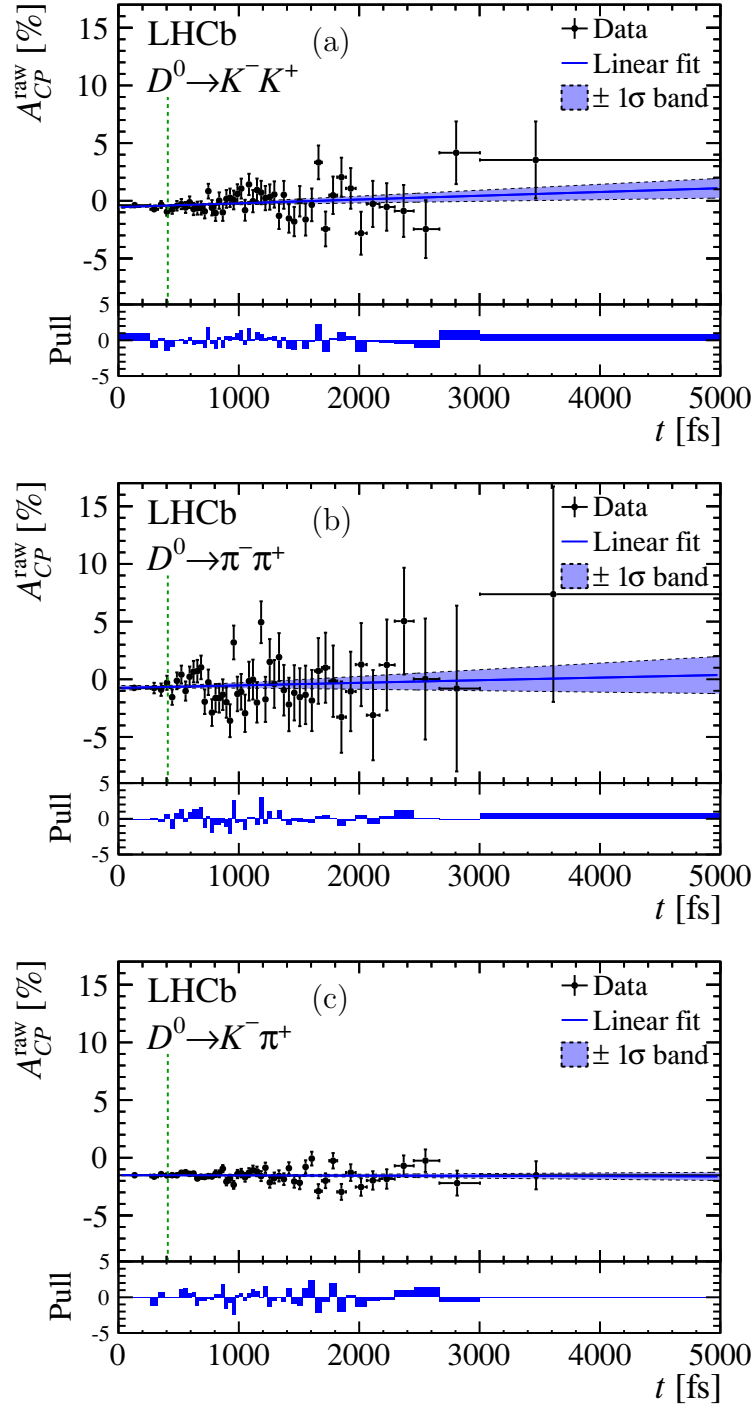


Figure 2. Raw CP asymmetry as function of D^0 decay time for (a) $D^0 \rightarrow K^- K^+$, (b) $D^0 \rightarrow \pi^- \pi^+$ and (c) $D^0 \rightarrow K^- \pi^+$ candidates. The results of the χ^2 fits are shown as blue, solid lines with the ± 1 standard-deviation (σ) bands indicated by the dashed lines. The green, dashed lines indicate one D^0 lifetime ($\tau = 410.1$ fs). Underneath each plot the pull in each time bin is shown.

Source of uncertainty	$D^0 \rightarrow K^- K^+$		$D^0 \rightarrow \pi^- \pi^+$	
	constant	scale	constant	scale
Mistag probability	0.006%	0.05	0.008%	0.05
Mistag asymmetry	0.016%		0.016%	
Time-dependent efficiency	0.010%		0.010%	
Detection and production asymmetries	0.010%		0.010%	
D^0 mass fit model	0.011%		0.007%	
D^0 decay-time resolution		0.09		0.07
$B^0-\bar{B}^0$ mixing	0.007%		0.007%	
Quadratic sum	0.026%	0.10	0.025%	0.09

Table 1. Contributions to the systematic uncertainty of $A_\Gamma(K^- K^+)$ and $A_\Gamma(\pi^- \pi^+)$. The constant and multiplicative scale uncertainties are given separately.

where the uncertainties are statistical only. The values for A_Γ are compatible with the assumption of no indirect CP violation. The fits have good p -values of 54.3% ($D^0 \rightarrow K^- K^+$), 30.8% ($D^0 \rightarrow \pi^- \pi^+$) and 14.5% ($D^0 \rightarrow K^- \pi^+$). The measured values for the raw time-integrated asymmetries, which are sensitive to direct CP violation, agree with those reported in ref. [13].

6 Systematic uncertainties and consistency checks

The contributions to the systematic uncertainty on A_Γ are listed in table 1. The largest contribution is due to the background coming from random combinations of muons and D^0 mesons. When the muon has the wrong charge compared to the real D^0 flavour, this is called a mistag. The mistag probability (ω) dilutes the observed asymmetry by a factor $(1 - 2\omega)$. This mistag probability is measured using $D^0 \rightarrow K^- \pi^+$ decays, exploiting the fact that the final state determines the flavour of the D^0 meson, except for an expected time-dependent wrong-sign fraction due to $D^0-\bar{D}^0$ mixing and doubly Cabibbo-suppressed decays. The mistag probability before correcting for wrong-sign decays is shown in figure 3. After subtracting the (time-dependent) wrong-sign ratio [3], the mistag probability as function of D^0 decay time is obtained. The mistag probability is small, with an average around 1%, but it is steeply increasing, reaching 5% at five D^0 lifetimes. This is due to the increase of the background fraction from real D^0 mesons from b -hadron decays combined with a muon from the opposite-side b -hadron decay. This random-muon background is reconstructed with an apparently longer lifetime. The time-dependent mistag probability is parameterised by an exponential function, which is used to determine the shift in A_Γ . The systematic uncertainty from this time-dependent mistag probability is 0.006% for the $D^0 \rightarrow K^- K^+$ and 0.008% for the $D^0 \rightarrow \pi^- \pi^+$ decay mode, with a supplementary, multiplicative scale uncertainty of 0.05 for both decay modes.

The mistag probabilities can potentially differ between positive and negative muons. Such a mistag asymmetry would give a direct contribution to the observed asymmetry.

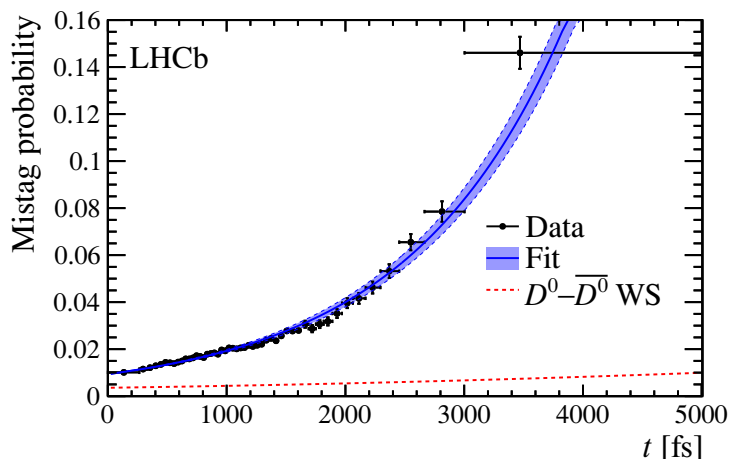


Figure 3. Mistag probability, before subtracting the contribution from wrong-sign (WS) decays, determined with $D^0 \rightarrow K^- \pi^+$ candidates. The result of the fit to the data points with an exponential function is overlaid (solid, blue line). The red, dashed line indicates the expected mistag contribution from WS decays.

The slope of the mistag asymmetry is also obtained from $D^0 \rightarrow K^- \pi^+$ decays. This slope is consistent with no time dependence, and its statistical uncertainty (0.016%) is included in the systematic uncertainty on A_Γ .

The selection of signal candidates, in particular the topological software trigger, is known to introduce a bias in the observed lifetime. Such a bias could be charge dependent, thus biasing the measurement of A_Γ . It is studied with the $D^0 \rightarrow K^- \pi^+$ sample and a sample of $D^- \rightarrow K^+ \pi^- \pi^-$ decays from semileptonic b -hadron decays. No asymmetry of the topological triggers in single-muon-triggered events is found within an uncertainty of 0.010%. This number is propagated as a systematic uncertainty.

The detection and production asymmetries introduce a constant offset in the raw time-dependent asymmetries. Since these asymmetries depend on the muon or b -hadron momentum, they can also introduce a time dependence in case the momentum spectrum varies between decay-time bins. This effect is tested by fitting the time-dependent asymmetry after weighting the events so that all decay-time bins have the same D^0 or muon momentum distribution. The observed shifts in A_Γ are within the statistical variations. The shift (0.010%) observed in the larger $D^0 \rightarrow K^- \pi^+$ sample, which has the same production asymmetry and larger detection asymmetry, is taken as a measure of the systematic uncertainty.

An inaccurate model of the mass distribution can introduce a bias in A_Γ . The effect on the observed asymmetries is studied by applying different models in the fits to the invariant mass distributions. For the signal, a sum of two Gaussian functions with and without an exponential tail, and for the background a first and a second-order polynomial are tested. The maximum variation from the default fit for each decay mode (0.011% for $D^0 \rightarrow K^- K^+$; 0.007% for $D^0 \rightarrow \pi^- \pi^+$) is taken as a systematic uncertainty on A_Γ .

The D^0 decay-time resolution affects the observed time scale, and therefore changes the measured value of A_Γ . For each decay mode, the resolution function is obtained from the simulation, which shows that for the majority of the signal (90%) the decay time is

measured with an RMS of about 103 fs. The remaining candidates (10%) are measured with an RMS of about 312 fs. The theoretical decay rates are convolved with the resolution functions in a large number of simulated experiments. The effect of the time resolution scales linearly with the size of A_Γ . The corresponding scale uncertainty on A_Γ is 0.09 for the $D^0 \rightarrow K^- K^+$ decay mode and 0.07 for the $D^0 \rightarrow \pi^- \pi^+$ decay mode. Decays where the muon gives the correct tag but the decay time is biased, e.g., when the muon originates from a τ lepton in the semileptonic b -hadron decay, are studied and found to be negligible.

About 40% of the muon-tagged D^0 decays originate from neutral B mesons [30]. Due to B^0 - \bar{B}^0 mixing the observed production asymmetry depends on the B^0 decay time [31]. A correlation between the B^0 and D^0 decay times may result in a shift in the measured value of A_Γ . The effect of this correlation, determined from simulation, together with a 1% B^0 production asymmetry [31, 32], is estimated to be a shift of 0.007% in the observed value of A_Γ . This is taken as systematic uncertainty.

Possible shifts in A_Γ coming from the 1.5 fs uncertainty on the world-average D^0 lifetime [28], from the uncertainty on the momentum scale and detector length scale [33, 34] and from potential biases in the fit method are negligible.

The scale uncertainty (cf. table 1) gives a small contribution to the overall systematic uncertainty, which depends on the true value of A_Γ . In order to present a single systematic uncertainty, the effect of the scale uncertainty is evaluated with a Neyman construction [35]. For each true value of A_Γ , the absolute size of the scale uncertainty is known and added in quadrature to the constant uncertainty. In this way, a confidence belt of observed values versus true values is constructed. This procedure gives a slightly asymmetric systematic uncertainty, which is $^{+0.026}_{-0.034}\%$ for the $D^0 \rightarrow K^- K^+$ decay channel and $^{+0.025}_{-0.033}\%$ for the $D^0 \rightarrow \pi^- \pi^+$ decay channel. Except for the contribution from the mass fit model, all contributions to the systematic uncertainty are fully correlated, resulting in an overall correlation coefficient of 89% between the systematic uncertainties of $A_\Gamma(K^- K^+)$ and $A_\Gamma(\pi^- \pi^+)$.

Additional checks have been performed to determine potential sensitivity of the measurements on the data-taking conditions, detector configuration, and analysis procedure. Changing to a finer decay-time binning yields compatible results. Potential effects on the measurement of A_Γ coming from detection asymmetries are expected to appear when dividing the data set by magnet polarity and data-taking period. Detection asymmetries originating from a left-right asymmetric detector change sign when reversing the magnet polarity. Similarly, during the two data-taking periods, detection asymmetries and production asymmetries might have changed due to different running conditions. As shown in figure 4, there is no significant variation of A_Γ across various configurations. Also splitting the data set according to the number of primary vertices or in bins of the B decay time does not show any deviation in the measured values of A_Γ .

7 Conclusions

The time-dependent CP asymmetries in $D^0 \rightarrow K^- K^+$ and $D^0 \rightarrow \pi^- \pi^+$ decays are measured using muon-tagged D^0 mesons originating from semileptonic b -hadron decays in the 3.0 fb^{-1} data set collected with the LHCb detector in 2011 and 2012. The asymmetries in

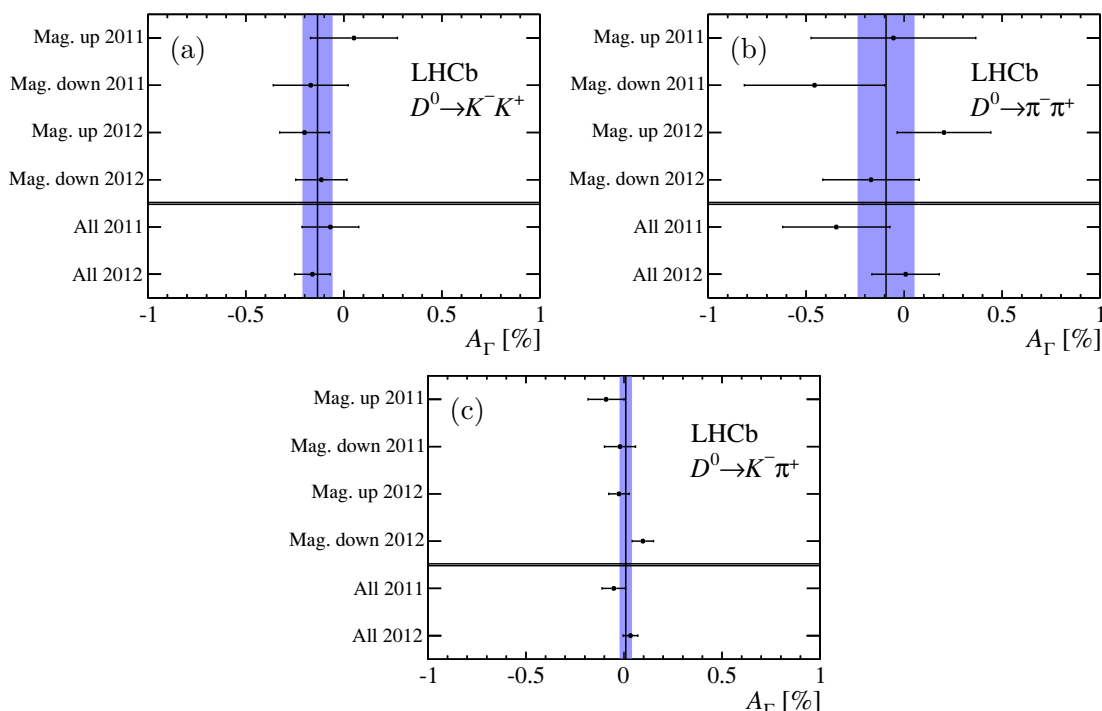


Figure 4. Measured values of A_Γ for different magnet polarities and data-taking periods for (a) $D^0 \rightarrow K^- K^+$, (b) $D^0 \rightarrow \pi^- \pi^+$ and (c) $D^0 \rightarrow K^- \pi^+$ decays. The vertical line and error band indicate the average A_Γ obtained from the combined data set. The error bars indicate the statistical uncertainty only.

the effective lifetimes are measured to be

$$A_\Gamma(K^- K^+) = (-0.134 \pm 0.077^{+0.026}_{-0.034}) \%,$$

$$A_\Gamma(\pi^- \pi^+) = (-0.092 \pm 0.145^{+0.025}_{-0.033}) \%,$$

where the first uncertainty is statistical and the second systematic. Assuming that indirect CP violation in D^0 decays is universal [10], and accounting for the correlation in the systematic uncertainties, the average of the two measurements becomes $A_\Gamma = (-0.125 \pm 0.073)\%$. The results in this paper are uncorrelated with the time-integrated asymmetries reported in ref. [13]. The results are consistent with other A_Γ measurements [1, 11, 12], and independent of the A_Γ measurements [11] from LHCb using D^0 mesons from $D^{*+} \rightarrow D^0 \pi^+$ decays. They are consistent with the hypothesis of no indirect CP violation in $D^0 \rightarrow K^- K^+$ and $D^0 \rightarrow \pi^- \pi^+$ decays.

Acknowledgments

We express our gratitude to our colleagues in the CERN accelerator departments for the excellent performance of the LHC. We thank the technical and administrative staff at the LHCb institutes. We acknowledge support from CERN and from the national agencies: CAPES, CNPq, FAPERJ and FINEP (Brazil); NSFC (China); CNRS/IN2P3 (France);

BMBF, DFG, HGF and MPG (Germany); INFN (Italy); FOM and NWO (The Netherlands); MNiSW and NCN (Poland); MEN/IFA (Romania); MinES and FANO (Russia); MinECo (Spain); SNSF and SER (Switzerland); NASU (Ukraine); STFC (United Kingdom); NSF (U.S.A.). The Tier1 computing centres are supported by IN2P3 (France), KIT and BMBF (Germany), INFN (Italy), NWO and SURF (The Netherlands), PIC (Spain), GridPP (United Kingdom). We are indebted to the communities behind the multiple open source software packages on which we depend. We are also thankful for the computing resources and the access to software R&D tools provided by Yandex LLC (Russia). Individual groups or members have received support from EPLANET, Marie Skłodowska-Curie Actions and ERC (European Union), Conseil général de Haute-Savoie, Labex ENIGMASS and OCEVU, Région Auvergne (France), RFBR (Russia), XuntaGal and GENCAT (Spain), Royal Society and Royal Commission for the Exhibition of 1851 (United Kingdom).

Open Access. This article is distributed under the terms of the Creative Commons Attribution License ([CC-BY 4.0](https://creativecommons.org/licenses/by/4.0/)), which permits any use, distribution and reproduction in any medium, provided the original author(s) and source are credited.

References

- [1] BABAR collaboration, J.P. Lees et al., *Measurement of D^0 - \bar{D}^0 mixing and CP violation in two-body D^0 decays*, *Phys. Rev. D* **87** (2013) 012004 [[arXiv:1209.3896](https://arxiv.org/abs/1209.3896)] [[INSPIRE](#)].
- [2] BABAR collaboration, P. del Amo Sanchez et al., *Measurement of D^0 - \bar{D}^0 mixing parameters using $D^0 \rightarrow K_S^0 \pi^+ \pi^-$ and $D^0 \rightarrow K_S^0 K^+ K^-$ decays*, *Phys. Rev. Lett.* **105** (2010) 081803 [[arXiv:1004.5053](https://arxiv.org/abs/1004.5053)] [[INSPIRE](#)].
- [3] LHCb collaboration, *Measurement of D^0 - \bar{D}^0 mixing parameters and search for CP violation using $D^0 \rightarrow K^+ \pi^-$ decays*, *Phys. Rev. Lett.* **111** (2013) 251801 [[arXiv:1309.6534](https://arxiv.org/abs/1309.6534)] [[INSPIRE](#)].
- [4] CDF collaboration, T.A. Aaltonen et al., *Observation of D^0 - \bar{D}^0 mixing using the CDF II detector*, *Phys. Rev. Lett.* **111** (2013) 231802 [[arXiv:1309.4078](https://arxiv.org/abs/1309.4078)] [[INSPIRE](#)].
- [5] BELLE collaboration, B.R. Ko et al., *Observation of D^0 - \bar{D}^0 mixing in e^+e^- collisions*, *Phys. Rev. Lett.* **112** (2014) 111801 [[arXiv:1401.3402](https://arxiv.org/abs/1401.3402)] [[INSPIRE](#)].
- [6] BELLE collaboration, T. Peng et al., *Measurement of D^0 - \bar{D}^0 mixing and search for indirect CP violation using $D^0 \rightarrow K_S^0 \pi^+ \pi^-$ decays*, *Phys. Rev. D* **89** (2014) 091103 [[arXiv:1404.2412](https://arxiv.org/abs/1404.2412)] [[INSPIRE](#)].
- [7] HEAVY FLAVOR AVERAGING GROUP (HFAG) collaboration, Y. Amhis et al., *Averages of b -hadron, c -hadron and τ -lepton properties as of summer 2014*, [arXiv:1412.7515](https://arxiv.org/abs/1412.7515) [[INSPIRE](#)].
- [8] S. Bianco, F.L. Fabbri, D. Benson and I. Bigi, *A Cicerone for the physics of charm*, *Riv. Nuovo Cim.* **26N7** (2003) 1 [[hep-ex/0309021](https://arxiv.org/abs/hep-ex/0309021)] [[INSPIRE](#)].
- [9] M. Bobrowski, A. Lenz, J. Riedl and J. Rohrwild, *How large can the SM contribution to CP violation in D^0 - \bar{D}^0 mixing be?*, *JHEP* **03** (2010) 009 [[arXiv:1002.4794](https://arxiv.org/abs/1002.4794)] [[INSPIRE](#)].
- [10] Y. Grossman, A.L. Kagan and Y. Nir, *New physics and CP violation in singly Cabibbo suppressed D decays*, *Phys. Rev. D* **75** (2007) 036008 [[hep-ph/0609178](https://arxiv.org/abs/hep-ph/0609178)] [[INSPIRE](#)].
- [11] LHCb collaboration, *Measurements of indirect CP asymmetries in $D^0 \rightarrow K^- K^+$ and $D^0 \rightarrow \pi^- \pi^+$ decays*, *Phys. Rev. Lett.* **112** (2014) 041801 [[arXiv:1310.7201](https://arxiv.org/abs/1310.7201)] [[INSPIRE](#)].

- [12] CDF collaboration, T.A. Aaltonen et al., *Measurement of indirect CP-violating asymmetries in $D^0 \rightarrow K^+K^-$ and $D^0 \rightarrow \pi^+\pi^-$ decays at CDF*, *Phys. Rev. D* **90** (2014) 111103 [[arXiv:1410.5435](#)] [[INSPIRE](#)].
- [13] LHCb collaboration, *Measurement of CP asymmetry in $D^0 \rightarrow K^-K^+$ and $D^0 \rightarrow \pi^-\pi^+$ decays*, *JHEP* **07** (2014) 041 [[arXiv:1405.2797](#)] [[INSPIRE](#)].
- [14] CDF collaboration, T. Aaltonen et al., *Measurement of CP-violating asymmetries in $D^0 \rightarrow \pi^+\pi^-$ and $D^0 \rightarrow K^+K^-$ decays at CDF*, *Phys. Rev. D* **85** (2012) 012009 [[arXiv:1111.5023](#)] [[INSPIRE](#)].
- [15] M. Gersabeck, M. Alexander, S. Borghi, V.V. Gligorov and C. Parkes, *On the interplay of direct and indirect CP violation in the charm sector*, *J. Phys. G* **39** (2012) 045005 [[arXiv:1111.6515](#)] [[INSPIRE](#)].
- [16] A.L. Kagan and M.D. Sokoloff, *Indirect CP violation and implications for $D^0-\bar{D}^0$ and $B_s-\bar{B}_s$ mixing*, *Phys. Rev. D* **80** (2009) 076008 [[arXiv:0907.3917](#)] [[INSPIRE](#)].
- [17] LHCb collaboration, *The LHCb detector at the LHC*, 2008 *JINST* **3** S08005 [[INSPIRE](#)].
- [18] LHCb collaboration, *LHCb detector performance*, *Int. J. Mod. Phys. A* **30** (2015) 1530022 [[arXiv:1412.6352](#)] [[INSPIRE](#)].
- [19] R. Aaij et al., *The LHCb trigger and its performance in 2011*, 2013 *JINST* **8** P04022 [[arXiv:1211.3055](#)] [[INSPIRE](#)].
- [20] T. Sjöstrand, S. Mrenna and P.Z. Skands, *PYTHIA 6.4 physics and manual*, *JHEP* **05** (2006) 026 [[hep-ph/0603175](#)] [[INSPIRE](#)].
- [21] T. Sjöstrand, S. Mrenna and P.Z. Skands, *A brief introduction to PYTHIA 8.1*, *Comput. Phys. Commun.* **178** (2008) 852 [[arXiv:0710.3820](#)] [[INSPIRE](#)].
- [22] I. Belyaev et al., *Handling of the generation of primary events in Gauss, the LHCb simulation framework*, *IEEE Nucl. Sci. Symp. Conf. Rec.* **1** (2010) 1155.
- [23] D.J. Lange, *The EvtGen particle decay simulation package*, *Nucl. Instrum. Meth. A* **462** (2001) 152 [[INSPIRE](#)].
- [24] P. Golonka and Z. Was, *PHOTOS Monte Carlo: A precision tool for QED corrections in Z and W decays*, *Eur. Phys. J. C* **45** (2006) 97 [[hep-ph/0506026](#)] [[INSPIRE](#)].
- [25] GEANT4 collaboration, J. Allison et al., *Geant4 developments and applications*, *IEEE Trans. Nucl. Sci.* **53** (2006) 270.
- [26] GEANT4 collaboration, S. Agostinelli et al., *GEANT4: A simulation toolkit*, *Nucl. Instrum. Meth. A* **506** (2003) 250 [[INSPIRE](#)].
- [27] LHCb collaboration, *The LHCb simulation application, Gauss: Design, evolution and experience*, *J. Phys. Conf. Ser.* **331** (2011) 032023 [[INSPIRE](#)].
- [28] PARTICLE DATA GROUP collaboration, K.A. Olive et al., *Review of particle physics*, *Chin. Phys. C* **38** (2014) 090001, <http://pdg.lbl.gov/>.
- [29] M. Pivk and F.R. Le Diberder, *sPlot: A statistical tool to unfold data distributions*, *Nucl. Instrum. Meth. A* **555** (2005) 356 [[physics/0402083](#)] [[INSPIRE](#)].
- [30] LHCb collaboration, *Search for direct CP violation in $D^0 \rightarrow h^-h^+$ modes using semileptonic B decays*, *Phys. Lett. B* **723** (2013) 33 [[arXiv:1303.2614](#)] [[INSPIRE](#)].

- [31] LHCb collaboration, *Measurement of the semileptonic CP asymmetry in B^0 - \bar{B}^0 mixing*, *Phys. Rev. Lett.* **114** (2015) 041601 [[arXiv:1409.8586](#)] [[INSPIRE](#)].
- [32] LHCb collaboration, *Measurement of the $\bar{B}^0 - B^0$ and $\bar{B}_s^0 - B_s^0$ production asymmetries in pp collisions at $\sqrt{s} = 7$ TeV*, *Phys. Lett. B* **739** (2014) 218 [[arXiv:1408.0275](#)] [[INSPIRE](#)].
- [33] R. Aaij et al., *Performance of the LHCb Vertex Locator*, *2014 JINST* **9** 09007 [[arXiv:1405.7808](#)] [[INSPIRE](#)].
- [34] LHCb collaboration, *Precision measurement of the B_s^0 - \bar{B}_s^0 oscillation frequency with the decay $B_s^0 \rightarrow D_s^- \pi^+$* , *New J. Phys.* **15** (2013) 053021 [[arXiv:1304.4741](#)] [[INSPIRE](#)].
- [35] J. Neyman, *Outline of a theory of statistical estimation based on the classical theory of probability*, *Phil. Trans. R. Soc. A* **236** (1937) 333.

The LHCb collaboration

R. Aaij⁴¹, B. Adeva³⁷, M. Adinolfi⁴⁶, A. Affolder⁵², Z. Ajaltouni⁵, S. Akar⁶, J. Albrecht⁹, F. Alessio³⁸, M. Alexander⁵¹, S. Ali⁴¹, G. Alkhazov³⁰, P. Alvarez Cartelle⁵³, A.A. Alves Jr^{25,38}, S. Amato², S. Amerio²², Y. Amhis⁷, L. An³, L. Anderlini^{17,g}, J. Anderson⁴⁰, R. Andreassen⁵⁷, M. Andreotti^{16,f}, J.E. Andrews⁵⁸, R.B. Appleby⁵⁴, O. Aquines Gutierrez¹⁰, F. Archilli³⁸, A. Artamonov³⁵, M. Artuso⁵⁹, E. Aslanides⁶, G. Auremma^{25,n}, M. Baalouch⁵, S. Bachmann¹¹, J.J. Back⁴⁸, A. Badalov³⁶, C. Baesso⁶⁰, W. Baldini¹⁶, R.J. Barlow⁵⁴, C. Barschel³⁸, S. Barsuk⁷, W. Barter³⁸, V. Batozskaya²⁸, V. Battista³⁹, A. Bay³⁹, L. Beaucourt⁴, J. Beddow⁵¹, F. Bedeschi²³, I. Bediaga¹, S. Belogurov³¹, I. Belyaev³¹, E. Ben-Haim⁸, G. Bencivenni¹⁸, S. Benson³⁸, J. Benton⁴⁶, A. Berezhnoy³², R. Bernet⁴⁰, A. Bertolin²², M.-O. Bettler⁴⁷, M. van Beuzekom⁴¹, A. Bien¹¹, S. Bifani⁴⁵, T. Bird⁵⁴, A. Bizzeti^{17,i}, T. Blake⁴⁸, F. Blanc³⁹, J. Blouw¹⁰, S. Blusk⁵⁹, V. Bocci²⁵, A. Bondar³⁴, N. Bondar^{30,38}, W. Bonivento¹⁵, S. Borghi⁵⁴, A. Borgia⁵⁹, M. Borsato⁷, T.J.V. Bowcock⁵², E. Bowen⁴⁰, C. Bozzi¹⁶, D. Brett⁵⁴, M. Britsch¹⁰, T. Britton⁵⁹, J. Brodzicka⁵⁴, N.H. Brook⁴⁶, A. Bursche⁴⁰, J. Buytaert³⁸, S. Cadetdu¹⁵, R. Calabrese^{16,f}, M. Calvi^{20,k}, M. Calvo Gomez^{36,p}, P. Campana¹⁸, D. Campora Perez³⁸, L. Capriotti⁵⁴, A. Carbone^{14,d}, G. Carboni^{24,l}, R. Cardinale^{19,38,j}, A. Cardini¹⁵, P. Carniti²⁰, L. Carson⁵⁰, K. Carvalho Akiba^{2,38}, RCM Casanova Mohr³⁶, G. Casse⁵², L. Cassina^{20,k}, L. Castillo Garcia³⁸, M. Cattaneo³⁸, Ch. Cauet⁹, G. Cavallero¹⁹, R. Cenci^{23,t}, M. Charles⁸, Ph. Charpentier³⁸, M. Chefdeville⁴, S. Chen⁵⁴, S.-F. Cheung⁵⁵, N. Chiapolini⁴⁰, M. Chrzasczcz^{40,26}, X. Cid Vidal³⁸, G. Ciezarek⁴¹, P.E.L. Clarke⁵⁰, M. Clemencic³⁸, H.V. Cliff⁴⁷, J. Closier³⁸, V. Coco³⁸, J. Cogan⁶, E. Cogneras⁵, V. Cogoni^{15,e}, L. Cojocariu²⁹, G. Collazuol²², P. Collins³⁸, A. Comerma-Montells¹¹, A. Contu^{15,38}, A. Cook⁴⁶, M. Coombes⁴⁶, S. Coquereau⁸, G. Corti³⁸, M. Corvo^{16,f}, I. Counts⁵⁶, B. Couturier³⁸, G.A. Cowan⁵⁰, D.C. Craik⁴⁸, A.C. Crocombe⁴⁸, M. Cruz Torres⁶⁰, S. Cunliffe⁵³, R. Currie⁵³, C. D'Ambrosio³⁸, J. Dalseno⁴⁶, P. David⁸, P.N.Y. David⁴¹, A. Davis⁵⁷, K. De Bruyn⁴¹, S. De Capua⁵⁴, M. De Cian¹¹, J.M. De Miranda¹, L. De Paula², W. De Silva⁵⁷, P. De Simone¹⁸, C.-T. Dean⁵¹, D. Decamp⁴, M. Deckenhoff⁹, L. Del Buono⁸, N. Déleage⁴, D. Derkach⁵⁵, O. Deschamps⁵, F. Dettori³⁸, B. Dey⁴⁰, A. Di Canto³⁸, A. Di Domenico²⁵, F. Di Ruscio²⁴, H. Dijkstra³⁸, S. Donleavy⁵², F. Dordei¹¹, M. Dorigo³⁹, A. Dosil Suárez³⁷, D. Dossett⁴⁸, A. Dovbnya⁴³, KD Dreimanis⁵², K. Dreimanis⁵², G. Dujany⁵⁴, F. Dupertuis³⁹, P. Durante⁶, R. Dzhelezhadin³⁵, A. Dziurda²⁶, A. Dzyuba³⁰, S. Easo^{49,38}, U. Egede⁵³, V. Egorychev³¹, S. Eidelman³⁴, S. Eisenhardt⁵⁰, U. Eitschberger⁹, R. Ekelhof⁹, L. Eklund⁵¹, I. El Rifai⁵, Ch. Elsasser⁴⁰, S. Ely⁵⁹, S. Esen¹¹, H.M. Evans⁴⁷, T. Evans⁵⁵, A. Falabella¹⁴, C. Färber¹¹, C. Farinelli⁴¹, N. Farley⁴⁵, S. Farry⁵², R. Fay⁵², D. Ferguson⁵⁰, V. Fernandez Albor³⁷, F. Ferreira Rodrigues¹, M. Ferro-Luzzi³⁸, S. Filippov³³, M. Fiore^{16,f}, M. Fiorini^{16,f}, M. Firlej²⁷, C. Fitzpatrick³⁹, T. Fiutowski²⁷, P. Fol⁵³, M. Fontana¹⁰, F. Fontanelli^{19,j}, R. Forty³⁸, O. Francisco², M. Frank³⁸, C. Frei³⁸, M. Frosini¹⁷, J. Fu^{21,38}, E. Furfaro^{24,l}, A. Gallas Torreira³⁷, D. Galli^{14,d}, S. Gallorini^{22,38}, S. Gambetta^{19,j}, M. Gandelman², P. Gandini⁵⁹, Y. Gao³, J. García Pardiñas³⁷, J. Garofoli⁵⁹, J. Garra Tico⁴⁷, L. Garrido³⁶, D. Gascon³⁶, C. Gaspar³⁸, U. Gastaldi¹⁶, R. Gauld⁵⁵, L. Gavardi⁹, G. Gazzoni⁵, A. Geraci^{21,v}, E. Gersabeck¹¹, M. Gersabeck⁵⁴, T. Gershon⁴⁸, Ph. Ghez⁴, A. Gianelle²², S. Giani³⁹, V. Gibson⁴⁷, L. Giubega²⁹, V.V. Gligorov³⁸, C. Göbel⁶⁰, D. Golubkov³¹, A. Golutvin^{53,31,38}, A. Gomes^{1,a}, C. Gotti^{20,k}, M. Grabalosa Gándara⁵, R. Graciani Diaz³⁶, L.A. Granado Cardoso³⁸, E. Graugés³⁶, E. Graverini⁴⁰, G. Graziani¹⁷, A. Grecu²⁹, E. Greening⁵⁵, S. Gregson⁴⁷, P. Griffith⁴⁵, L. Grillo¹¹, O. Grünberg⁶³, B. Gui⁵⁹, E. Gushchin³³, Yu. Guz^{35,38}, T. Gys³⁸, C. Hadjivasiliou⁵⁹, G. Haefeli³⁹, C. Haen³⁸, S.C. Haines⁴⁷, S. Hall⁵³, B. Hamilton⁵⁸, T. Hampson⁴⁶, X. Han¹¹, S. Hansmann-Menzemer¹¹, N. Harnew⁵⁵, S.T. Harnew⁴⁶, J. Harrison⁵⁴, J. He³⁸, T. Head³⁹, V. Heijne⁴¹, K. Hennessy⁵², P. Henrard⁵, L. Henry⁸, J.A. Hernando Morata³⁷,

E. van Herwijnen³⁸, M. Heß⁶³, A. Hicheur², D. Hill⁵⁵, M. Hoballah⁵, C. Hombach⁵⁴, W. Hulsbergen⁴¹, T. Humair⁵³, N. Hussain⁵⁵, D. Hutchcroft⁵², D. Hynds⁵¹, M. Idzik²⁷, P. Ilten⁵⁶, R. Jacobsson³⁸, A. Jaeger¹¹, J. Jalocha⁵⁵, E. Jans⁴¹, A. Jawahery⁵⁸, F. Jing³, M. John⁵⁵, D. Johnson³⁸, C.R. Jones⁴⁷, C. Joram³⁸, B. Jost³⁸, N. Jurik⁵⁹, S. Kandybei⁴³, W. Kanso⁶, M. Karacson³⁸, T.M. Karbach³⁸, S. Karodia⁵¹, M. Kelsey⁵⁹, I.R. Kenyon⁴⁵, M. Kenzie³⁸, T. Ketel⁴², B. Khanji^{20,38,k}, C. Khurewathanakul³⁹, S. Klaver⁵⁴, K. Klimaszewski²⁸, O. Kochebina⁷, M. Kolpin¹¹, I. Komarov³⁹, R.F. Koopman⁴², P. Koppenburg^{41,38}, M. Korolev³², L. Kravchuk³³, K. Kreplin¹¹, M. Kreps⁴⁸, G. Krocker¹¹, P. Krokovny³⁴, F. Kruse⁹, W. Kucewicz^{26,o}, M. Kucharczyk^{20,k}, V. Kudryavtsev³⁴, K. Kurek²⁸, T. Kvaratskheliya³¹, V.N. La Thi³⁹, D. Lacarrere³⁸, G. Lafferty⁵⁴, A. Lai¹⁵, D. Lambert⁵⁰, R.W. Lambert⁴², G. Lanfranchi¹⁸, C. Langenbruch⁴⁸, B. Langhans³⁸, T. Latham⁴⁸, C. Lazzeroni⁴⁵, R. Le Gac⁶, J. van Leerdam⁴¹, J.-P. Lees⁴, R. Lefèvre⁵, A. Leflat³², J. Lefrançois⁷, O. Leroy⁶, T. Lesiak²⁶, B. Leverington¹¹, Y. Li⁷, T. Likhomanenko⁶⁴, M. Liles⁵², R. Lindner³⁸, C. Linn³⁸, F. Lionetto⁴⁰, B. Liu¹⁵, S. Lohn³⁸, I. Longstaff⁵¹, J.H. Lopes², P. Lowdon⁴⁰, D. Lucchesi^{22,r}, H. Luo⁵⁰, A. Lupato²², E. Luppi^{16,f}, O. Lupton⁵⁵, F. Machefert⁷, I.V. Machikhiliyan³¹, F. Maciuc²⁹, O. Maev³⁰, S. Malde⁵⁵, A. Malinin⁶⁴, G. Manca^{15,e}, G. Mancinelli⁶, P. Manning⁵⁹, A. Mapelli³⁸, J. Maratas⁵, J.F. Marchand⁴, U. Marconi¹⁴, C. Marin Benito³⁶, P. Marino^{23,t}, R. Märki³⁹, J. Marks¹¹, G. Martellotti²⁵, M. Martinelli³⁹, D. Martinez Santos⁴², F. Martinez Vidal⁶⁶, D. Martins Tostes², A. Massafferri¹, R. Matev³⁸, Z. Mathe³⁸, C. Matteuzzi²⁰, A. Mauri⁴⁰, B. Maurin³⁹, A. Mazurov⁴⁵, M. McCann⁵³, J. McCarthy⁴⁵, A. McNab⁵⁴, R. McNulty¹², B. McSkelly⁵², B. Meadows⁵⁷, F. Meier⁹, M. Meissner¹¹, M. Merk⁴¹, D.A. Milanese⁶², M.-N. Minard⁴, N. Moggi¹⁴, J. Molina Rodriguez⁶⁰, S. Monteil⁵, M. Morandin²², P. Morawski²⁷, A. Mordà⁶, M.J. Morello^{23,t}, J. Moron²⁷, A.-B. Morris⁵⁰, R. Mountain⁵⁹, F. Muheim⁵⁰, K. Müller⁴⁰, M. Mussini¹⁴, B. Muster³⁹, P. Naik⁴⁶, T. Nakada³⁹, R. Nandakumar⁴⁹, I. Nasteva², M. Needham⁵⁰, N. Neri²¹, S. Neubert¹¹, N. Neufeld³⁸, M. Neuner¹¹, A.D. Nguyen³⁹, T.D. Nguyen³⁹, C. Nguyen-Mau^{39,q}, M. Nicol⁷, V. Niess⁵, R. Niet⁹, N. Nikitin³², T. Nikodem¹¹, A. Novoselov³⁵, D.P. O'Hanlon⁴⁸, A. Oblakowska-Mucha²⁷, V. Obraztsov³⁵, S. Ogilvy⁵¹, O. Okhrimenko⁴⁴, R. Oldeman^{15,e}, C.J.G. Onderwater⁶⁷, B. Osorio Rodrigues¹, J.M. Otalora Goicochea², A. Otto³⁸, P. Owen⁵³, A. Oyanguren⁶⁶, B.K. Pal⁵⁹, A. Palano^{13,c}, F. Palombo^{21,u}, M. Palutan¹⁸, J. Panman³⁸, A. Papanestis⁴⁹, M. Pappagallo⁵¹, L.L. Pappalardo^{16,f}, C. Parkes⁵⁴, C.J. Parkinson^{9,45}, G. Passaleva¹⁷, G.D. Patel⁵², M. Patel⁵³, C. Patrignani^{19,j}, A. Pearce^{54,49}, A. Pellegrino⁴¹, G. Penso^{25,m}, M. Pepe Altarelli³⁸, S. Perazzini^{14,d}, P. Perret⁵, L. Pescatore⁴⁵, E. Pesen⁶⁸, K. Petridis⁴⁶, A. Petrolini^{19,j}, E. Picatoste Olloqui³⁶, B. Pietrzyk⁴, T. Pilar⁴⁸, D. Pinci²⁵, A. Pistone¹⁹, S. Playfer⁵⁰, M. Plo Casasus³⁷, F. Polci⁸, A. Poluektov^{48,34}, I. Polyakov³¹, E. Polycarpo², A. Popov³⁵, D. Popov¹⁰, B. Popovici²⁹, C. Potterat², E. Price⁴⁶, J.D. Price⁵², J. Prisciandaro³⁹, A. Pritchard⁵², C. Prouve⁴⁶, V. Pugatch⁴⁴, A. Puig Navarro³⁹, G. Punzi^{23,s}, W. Qian⁴, R. Quagliani^{7,46}, B. Rachwal²⁶, J.H. Rademacker⁴⁶, B. Rakotomiamanana³⁹, M. Rama²³, M.S. Rangel², I. Raniuk⁴³, N. Rauschmayr³⁸, G. Raven⁴², F. Redi⁵³, S. Reichert⁵⁴, M.M. Reid⁴⁸, A.C. dos Reis¹, S. Ricciardi⁴⁹, S. Richards⁴⁶, M. Rihl³⁸, K. Rinnert⁵², V. Rives Molina³⁶, P. Robbe⁷, A.B. Rodrigues¹, E. Rodrigues⁵⁴, P. Rodriguez Perez⁵⁴, S. Roiser³⁸, V. Romanovsky³⁵, A. Romero Vidal³⁷, M. Rotondo²², J. Rouvinet³⁹, T. Ruf³⁸, H. Ruiz³⁶, P. Ruiz Valls⁶⁶, J.J. Saborido Silva³⁷, N. Sagidova³⁰, P. Sail⁵¹, B. Saitta^{15,e}, V. Salustino Guimaraes², C. Sanchez Mayordomo⁶⁶, B. Sanmartin Sedes³⁷, R. Santacesaria²⁵, C. Santamarina Rios³⁷, E. Santovetti^{24,l}, A. Sarti^{18,m}, C. Satriano^{25,n}, A. Satta²⁴, D.M. Saunders⁴⁶, D. Savrina^{31,32}, M. Schiller³⁸, H. Schindler³⁸, M. Schlupp⁹, M. Schmelling¹⁰, B. Schmidt³⁸, O. Schneider³⁹, A. Schopper³⁸, M.-H. Schune⁷, R. Schwemmer³⁸, B. Sciascia¹⁸, A. Sciubba^{25,m}, A. Semennikov³¹, I. Sepp⁵³, N. Serra⁴⁰, J. Serrano⁶, L. Sestini²², P. Seyfert¹¹,

M. Shapkin³⁵, I. Shapoval^{16,43,f}, Y. Shcheglov³⁰, T. Shears⁵², L. Shekhtman³⁴, V. Shevchenko⁶⁴, A. Shires⁹, R. Silva Coutinho⁴⁸, G. Simi²², M. Sirendi⁴⁷, N. Skidmore⁴⁶, I. Skillicorn⁵¹, T. Skwarnicki⁵⁹, N.A. Smith⁵², E. Smith^{55,49}, E. Smith⁵³, J. Smith⁴⁷, M. Smith⁵⁴, H. Snoek⁴¹, M.D. Sokoloff⁵⁷, F.J.P. Soler⁵¹, F. Soomro³⁹, D. Souza⁴⁶, B. Souza De Paula², B. Spaan⁹, P. Spradlin⁵¹, S. Sridharan³⁸, F. Stagni³⁸, M. Stahl¹¹, S. Stahl³⁸, O. Steinkamp⁴⁰, O. Stenyakin³⁵, F. Sterpka⁵⁹, S. Stevenson⁵⁵, S. Stoica²⁹, S. Stone⁵⁹, B. Storaci⁴⁰, S. Stracka^{23,t}, M. Straticiuc²⁹, U. Straumann⁴⁰, R. Stroili²², L. Sun⁵⁷, W. Sutcliffe⁵³, K. Swientek²⁷, S. Swientek⁹, V. Syropoulos⁴², M. Szczekowski²⁸, P. Szczypka^{39,38}, T. Szumlak²⁷, S. T'Jampens⁴, M. Teklishyn⁷, G. Tellarini^{16,f}, F. Teubert³⁸, C. Thomas⁵⁵, E. Thomas³⁸, J. van Tilburg⁴¹, V. Tisserand⁴, M. Tobin³⁹, J. Todd⁵⁷, S. Tolk⁴², L. Tomassetti^{16,f}, D. Tonelli³⁸, S. Topp-Joergensen⁵⁵, N. Torr⁵⁵, E. Tournefier⁴, S. Tourneur³⁹, K. Trabelsi³⁹, M.T. Tran³⁹, M. Tresch⁴⁰, A. Trisovic³⁸, A. Tsaregorodtsev⁶, P. Tsopelas⁴¹, N. Tuning^{41,38}, M. Ubeda Garcia³⁸, A. Ukleja²⁸, A. Ustyuzhanin⁶⁵, U. Uwer¹¹, C. Vacca^{15,e}, V. Vagnoni¹⁴, G. Valenti¹⁴, A. Vallier⁷, R. Vazquez Gomez¹⁸, P. Vazquez Regueiro³⁷, C. Vázquez Sierra³⁷, S. Vecchi¹⁶, J.J. Velthuis⁴⁶, M. Veltri^{17,h}, G. Veneziano³⁹, M. Vesterinen¹¹, J.V. Viana Barbosa³⁸, B. Viaud⁷, D. Vieira², M. Vieites Diaz³⁷, X. Vilasis-Cardona^{36,p}, A. Vollhardt⁴⁰, D. Volyanskyy¹⁰, D. Voong⁴⁶, A. Vorobyev³⁰, V. Vorobyev³⁴, C. Voß⁶³, J.A. de Vries⁴¹, R. Waldi⁶³, C. Wallace⁴⁸, R. Wallace¹², J. Walsh²³, S. Wandernoth¹¹, J. Wang⁵⁹, D.R. Ward⁴⁷, N.K. Watson⁴⁵, D. Websdale⁵³, M. Whitehead⁴⁸, D. Wiedner¹¹, G. Wilkinson^{55,38}, M. Wilkinson⁵⁹, M.P. Williams⁴⁵, M. Williams⁵⁶, H.W. Wilschut⁶⁷, F.F. Wilson⁴⁹, J. Wimberley⁵⁸, J. Wishahi⁹, W. Wislicki²⁸, M. Witek²⁶, G. Wormser⁷, S.A. Wotton⁴⁷, S. Wright⁴⁷, K. Wyllie³⁸, Y. Xie⁶¹, Z. Xing⁵⁹, Z. Xu³⁹, Z. Yang³, X. Yuan³⁴, O. Yushchenko³⁵, M. Zangoli¹⁴, M. Zavertyaev^{10,b}, L. Zhang³, W.C. Zhang¹², Y. Zhang³, A. Zhelezov¹¹, A. Zhokhov³¹ and L. Zhong³

¹ Centro Brasileiro de Pesquisas Físicas (CBPF), Rio de Janeiro, Brazil

² Universidade Federal do Rio de Janeiro (UFRJ), Rio de Janeiro, Brazil

³ Center for High Energy Physics, Tsinghua University, Beijing, China

⁴ LAPP, Université de Savoie, CNRS/IN2P3, Annecy-Le-Vieux, France

⁵ Clermont Université, Université Blaise Pascal, CNRS/IN2P3, LPC, Clermont-Ferrand, France

⁶ CPPM, Aix-Marseille Université, CNRS/IN2P3, Marseille, France

⁷ LAL, Université Paris-Sud, CNRS/IN2P3, Orsay, France

⁸ LPNHE, Université Pierre et Marie Curie, Université Paris Diderot, CNRS/IN2P3, Paris, France

⁹ Fakultät Physik, Technische Universität Dortmund, Dortmund, Germany

¹⁰ Max-Planck-Institut für Kernphysik (MPIK), Heidelberg, Germany

¹¹ Physikalisches Institut, Ruprecht-Karls-Universität Heidelberg, Heidelberg, Germany

¹² School of Physics, University College Dublin, Dublin, Ireland

¹³ Sezione INFN di Bari, Bari, Italy

¹⁴ Sezione INFN di Bologna, Bologna, Italy

¹⁵ Sezione INFN di Cagliari, Cagliari, Italy

¹⁶ Sezione INFN di Ferrara, Ferrara, Italy

¹⁷ Sezione INFN di Firenze, Firenze, Italy

¹⁸ Laboratori Nazionali dell'INFN di Frascati, Frascati, Italy

¹⁹ Sezione INFN di Genova, Genova, Italy

²⁰ Sezione INFN di Milano Bicocca, Milano, Italy

²¹ Sezione INFN di Milano, Milano, Italy

²² Sezione INFN di Padova, Padova, Italy

²³ Sezione INFN di Pisa, Pisa, Italy

²⁴ Sezione INFN di Roma Tor Vergata, Roma, Italy

²⁵ Sezione INFN di Roma La Sapienza, Roma, Italy

²⁶ Henryk Niewodniczanski Institute of Nuclear Physics Polish Academy of Sciences, Kraków, Poland

- ²⁷ AGH — University of Science and Technology, Faculty of Physics and Applied Computer Science, Kraków, Poland
- ²⁸ National Center for Nuclear Research (NCBJ), Warsaw, Poland
- ²⁹ Horia Hulubei National Institute of Physics and Nuclear Engineering, Bucharest-Magurele, Romania
- ³⁰ Petersburg Nuclear Physics Institute (PNPI), Gatchina, Russia
- ³¹ Institute of Theoretical and Experimental Physics (ITEP), Moscow, Russia
- ³² Institute of Nuclear Physics, Moscow State University (SINP MSU), Moscow, Russia
- ³³ Institute for Nuclear Research of the Russian Academy of Sciences (INR RAN), Moscow, Russia
- ³⁴ Budker Institute of Nuclear Physics (SB RAS) and Novosibirsk State University, Novosibirsk, Russia
- ³⁵ Institute for High Energy Physics (IHEP), Protvino, Russia
- ³⁶ Universitat de Barcelona, Barcelona, Spain
- ³⁷ Universidad de Santiago de Compostela, Santiago de Compostela, Spain
- ³⁸ European Organization for Nuclear Research (CERN), Geneva, Switzerland
- ³⁹ Ecole Polytechnique Fédérale de Lausanne (EPFL), Lausanne, Switzerland
- ⁴⁰ Physik-Institut, Universität Zürich, Zürich, Switzerland
- ⁴¹ Nikhef National Institute for Subatomic Physics, Amsterdam, The Netherlands
- ⁴² Nikhef National Institute for Subatomic Physics and VU University Amsterdam, Amsterdam, The Netherlands
- ⁴³ NSC Kharkiv Institute of Physics and Technology (NSC KIPT), Kharkiv, Ukraine
- ⁴⁴ Institute for Nuclear Research of the National Academy of Sciences (KINR), Kyiv, Ukraine
- ⁴⁵ University of Birmingham, Birmingham, United Kingdom
- ⁴⁶ H.H. Wills Physics Laboratory, University of Bristol, Bristol, United Kingdom
- ⁴⁷ Cavendish Laboratory, University of Cambridge, Cambridge, United Kingdom
- ⁴⁸ Department of Physics, University of Warwick, Coventry, United Kingdom
- ⁴⁹ STFC Rutherford Appleton Laboratory, Didcot, United Kingdom
- ⁵⁰ School of Physics and Astronomy, University of Edinburgh, Edinburgh, United Kingdom
- ⁵¹ School of Physics and Astronomy, University of Glasgow, Glasgow, United Kingdom
- ⁵² Oliver Lodge Laboratory, University of Liverpool, Liverpool, United Kingdom
- ⁵³ Imperial College London, London, United Kingdom
- ⁵⁴ School of Physics and Astronomy, University of Manchester, Manchester, United Kingdom
- ⁵⁵ Department of Physics, University of Oxford, Oxford, United Kingdom
- ⁵⁶ Massachusetts Institute of Technology, Cambridge, MA, United States
- ⁵⁷ University of Cincinnati, Cincinnati, OH, United States
- ⁵⁸ University of Maryland, College Park, MD, United States
- ⁵⁹ Syracuse University, Syracuse, NY, United States
- ⁶⁰ Pontifícia Universidade Católica do Rio de Janeiro (PUC-Rio), Rio de Janeiro, Brazil, associated to ²
- ⁶¹ Institute of Particle Physics, Central China Normal University, Wuhan, Hubei, China, associated to ³
- ⁶² Departamento de Física, Universidad Nacional de Colombia, Bogota, Colombia, associated to ⁸
- ⁶³ Institut für Physik, Universität Rostock, Rostock, Germany, associated to ¹¹
- ⁶⁴ National Research Centre Kurchatov Institute, Moscow, Russia, associated to ³¹
- ⁶⁵ Yandex School of Data Analysis, Moscow, Russia, associated to ³¹
- ⁶⁶ Instituto de Física Corpuscular (IFIC), Universitat de Valencia-CSIC, Valencia, Spain, associated to ³⁶
- ⁶⁷ Van Swinderen Institute, University of Groningen, Groningen, The Netherlands, associated to ⁴¹
- ⁶⁸ Celal Bayar University, Manisa, Turkey, associated to ³⁸
- ^a Universidade Federal do Triângulo Mineiro (UFTM), Uberaba-MG, Brazil
- ^b P.N. Lebedev Physical Institute, Russian Academy of Science (LPI RAS), Moscow, Russia

- ^c *Università di Bari, Bari, Italy*
- ^d *Università di Bologna, Bologna, Italy*
- ^e *Università di Cagliari, Cagliari, Italy*
- ^f *Università di Ferrara, Ferrara, Italy*
- ^g *Università di Firenze, Firenze, Italy*
- ^h *Università di Urbino, Urbino, Italy*
- ⁱ *Università di Modena e Reggio Emilia, Modena, Italy*
- ^j *Università di Genova, Genova, Italy*
- ^k *Università di Milano Bicocca, Milano, Italy*
- ^l *Università di Roma Tor Vergata, Roma, Italy*
- ^m *Università di Roma La Sapienza, Roma, Italy*
- ⁿ *Università della Basilicata, Potenza, Italy*
- ^o *AGH — University of Science and Technology,
Faculty of Computer Science, Electronics and Telecommunications, Kraków, Poland*
- ^p *LIFAEELS, La Salle, Universitat Ramon Llull, Barcelona, Spain*
- ^q *Hanoi University of Science, Hanoi, Viet Nam*
- ^r *Università di Padova, Padova, Italy*
- ^s *Università di Pisa, Pisa, Italy*
- ^t *Scuola Normale Superiore, Pisa, Italy*
- ^u *Università degli Studi di Milano, Milano, Italy*
- ^v *Politecnico di Milano, Milano, Italy*